Semnan University

Journal of Heat and Mass Transfer Research

Journal homepage: http://jhmtr.journals.semnan.ac.ir

Thermodynamic analysis of a magnetohydrodyamic oldroyd 8-constant fluid in a vertical channel with heat source and slippage

Gbadeyan Jacob Abiodun, Yusuf Tunde Abdulkadir*

Department of Mathematics, University of Ilorin, Ilorin, Kwara State, Nigeria.

PAPER INFO

History:

Submitted 2017-04-22
Revised 2017-10-06
Accepted 2017-10-12

Keywords:

Oldroyd 8-constant fluid;
Entropy generation;
Buoyancy effect;
Heat source;
Bejan number

A B S T R A C T

This study carried out a thermodynamic analysis of the steady-state flow and heat transfer of an Oldroyd 8-constant fluid, with consideration for the effects of heat source, velocity slip, and buoyancy force under a transverse magnetic field. A model for momentum and energy balance was numerically solved using the method of weighted residuals, and associated residuals were minimized using the partition method. The results were compared with those derived using the built-in numerical solver of MAPLE 18 to validate the method used, and the convergence of the method was determined. The results of the momentum and energy balance model were then used to compute the entropy generation rate and the irreversibility ratio. The effects of control parameters such as non-Newtonian fluid parameters, slip parameters, the Grashoff, Brinkmann, and Hartmann numbers, and heat source on non-dimensional velocity, temperature, entropy generation, and irreversibility were graphically represented. The findings revealed that the irreversibility due to fluid friction dominates over heat transfer when non-Newtonian fluid parameter α_1 is kept constant at various values of α_2, whereas the irreversibility due to heat transfer dominates over fluid friction when α_2 is kept constant at various values of α_1.

DOI: 10.22075/jhmtr.2017.1503.1100

1. Introduction

Non-Newtonian fluid mechanics is a field of study that has grown in prominence and importance over time. In recent years, efforts have been devoted to the study of non-Newtonian fluid flow mainly because of the many applications of such phenomenon in petroleum drilling, bioengineering, and food and paper manufacturing. A non-Newtonian fluid is a class of fluid with properties that differ in many ways from those of Newtonian fluids. The viscosity of non-Newtonian fluids, for instance, depends on shear rate. Additionally, many models used to describe the non-Newtonian behavior exhibited by certain fluids feature governing equations that are of higher order and are much more complicated than Navier–Stokes equations. The resultant non-linear equations are difficult to solve given their considerable complexity and have therefore posed tremendous challenges to researchers in engineering, applied mathematics, and computational mathematics. Most of the mathematical models used to describe the physical flow behavior of non-Newtonian fluids can be grouped into three classes: (a) the rate class, (b) the differential class, and (c) the integral class. Differential models are used to predict normal stress and shear thinning/thickening properties. In the integral type model, the stress is given by one or more integrals of deformation history, while the rate type model are used to describe the response of fluid that have slight dependence of the stress on the history of the relative deformation gradient. Unlike the differential and the integral types whose constitutive equations are explicit of the stress tensor, the rate type is implicit in the stress tensor. The most common rate-type fluid model is the

Corresponding Author : bDepartment of Mathematics, University of Ilorin,Ilorin, Kwara State, Nigeria
Email : tundeayusuf04@gmail.com

Oldroyd model proposed by Oldroyd [1]. This model differs from differential models in terms of effectiveness in predicting normal stress and shear thinning/thickening properties and measuring relaxation and retardation times. The simplest subclass of rate-type fluid models is the Maxwell fluid model, which can be described only in terms of the fluid's relaxation time. Another subclass is the convected Jeffrey model, which is also known as the Oldroyd B model and is used to predict the effects of relaxation and retardation times. A generalized subclass of the Oldroyd model is the Oldroyd 8-constant model—a non-Newtonian fluid representation that has received relatively less attention from researchers. To address this gap, the present study employed an Oldroyd 8-constant fluid model, which is a generalized class because it is used to predict normal stress properties, shear thinning/thickening properties, and many other characteristics [2]. It also identifies the rheological characteristics of unidirectional steady flow. Other researchers have similarly investigated Oldroyd fluids. Hayat et al. [3], for example, discussed the flow of an Oldroyd 8-constant fluid subjected to a magnetic field using homotopy analysis. Hayat et al. [4] examined the magnetohydrodynamic (MHD) flow of an Oldroyd 6-constant fluid. Khan et al. [5] inquired into the effects of slip on shearing flow in a porous medium, and Ellahi et al. [6] explored the analytical solution of the non-linear flow problem of an Oldroyd 8-constant fluid. Furthermore, Baris [7] investigated the flow of an Oldroyd 8-constant fluid in a convergent channel. Using homotopy analysis, Khan et al. [8] examined heat transfer from the steady flow of an Oldroyd 8-constant fluid into a suddenly moving plate. In other studies [9,10], the authors numerically investigated partial slippage on the MHD flow of an Oldroyd 8-constant fluid.

Numerous researchers have also delved into the various flow behaviors of viscous fluids under slip conditions [11–14]. However, little effort has been devoted to using the Oldroyd fluid model to elucidate velocity at boundaries. Some of the few studies in this regard are those conducted by Khan et al. [9,10], as well as that carried out by Hayat et al. [5], who investigated the effects of slip conditions on the flow of an Oldroyd 6-constant fluid.

Many scholars have likewise been considerably interested in entropy generation given its vast applications in minimizing the wastage of scarce resources [15]. Notable studies on this issue include those of Bejan [16,17],who discussed the second law analysis of heat transfer, thereby carrying out analysis of entropy generation. Vyas and Rai [18] examined the entropy regime of radiative MHD couette flow in a channel with a natural permeable base. Das and Jana [11] examined the entropy generation due to MHD flow in a porous channel characterized by Navier slip conditions. Adesanya [19–22] studied the entropy generation of couple stress fluid and third-grade fluid that flow through a channel. The effects of buoyancy on the unsteady MHD flow of a reactive third-grade fluid with asymmetric convective cooling were explored by Eegunjobi and Makinde [14]. Adesanya [21] delved into the second law analysis of third-grade fluids with variable viscosity. Gbadeyan et al. [12,13] and Ajibade et al. [23] are also among the researchers who have investigated entropy generation during various fluid flows. To the best of our knowledge, entropy generation during the flow of an Oldroyd 8-constant fluid has not been examined. This analysis constituted the main goal of the current research.

2. Mathematical Formulation

Let us consider the steady flow of an electrically conducting viscous fluid between two vertical and parallel plates of infinite lengths aty = 0 and y = h with non-uniform temperature under the combined effects of buoyancy and velocity slip (Fig. 1). The Cauchy stress tensor τ for an incompressible Oldroyd 8-constant fluid is expressed, following [2], thus:

$$\tau = -pI + S \tag{1}$$

where p is the pressure,Idenotesthe identity tensor, and Srepresentsthe extra stress tensor, expressed as

$$\begin{aligned} S + \lambda_1 \frac{DS}{Dt} + \frac{\lambda_3}{2}(SA_1 + A_1S) + \frac{\lambda_5}{2}(trS)A_1 \\ + \frac{\lambda_6}{2}[trSA_1]I \\ = \mu\left(A_1 + \lambda_2 \frac{DA_1}{Dt} + \lambda_4 {A_1}^2 \right. \\ \left. + \frac{\lambda_7}{2}\left[tr\left({A_1}^2\right)\right]I\right) \end{aligned} \tag{2}$$

where A_1 is the Revlin–Ericksen tensor, μ is the coefficient of shear viscosity, and λ_i (i = 1,2,3 ... 7)represents the material constants. Revlin–Ericksen tensor A_1 is defined as

$$A_1 = L + L^T \; and \; L = gradV \tag{3}$$

and the contravariant derivative $\frac{D}{Dt}$ for steady flow is given as

$$\begin{aligned} \frac{DS}{Dt} = \frac{dS}{dt} - LS - SL^T and \; \frac{DA_1}{Dt} \\ = \frac{dA_1}{dt} - LA_1 - A_1L^T \end{aligned} \tag{4}$$

where $\frac{d}{dt}$ is the material time derivative.

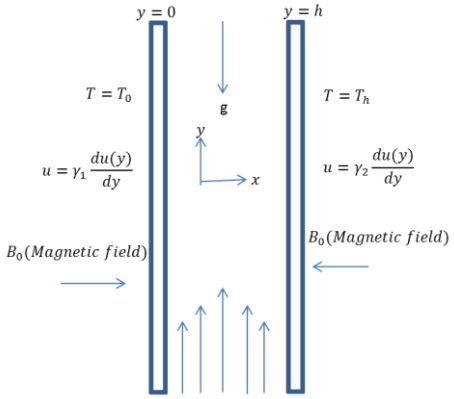

Fig. 1. Geometry of the model

An Oldroyd 8-constant fluid is the general case of Newtonian, Maxwell, second-grade, and Oldroyd 3- and 6- constant fluids. When λ_i are set to zero for $(i = 1,2,3 \ldots 7)$, the Oldroyd 8-constant model is reduced to a Newtonian fluid model, but when $\lambda_1 \neq 0, \lambda_i = 0$ $(i = 2,3..7)$, the model is converted into a Maxwell fluid model. The model becomes a second-grade fluid model at $\lambda_1 = 0, \mu\lambda_2 = \alpha_1, \lambda_i = 0$ $(i = 3,4..7)$ and is reduced toan Oldroyd 3-constant fluid model at $\lambda_1 \neq 0 \neq \lambda_2, \lambda_i = 0$ $(i = 3,4..7)$. Finally, the model is reduced to an Oldroyd 6-constant fluid model when $\lambda_6 = 0 = \lambda_7$ [3]. We assume a stress tensor, velocity, and temperature of the form

$$S = \begin{pmatrix} S_{xx} & S_{xy} & S_{xz} \\ S_{yx} & S_{yy} & S_{yz} \\ S_{zx} & S_{zy} & S_{zz} \end{pmatrix}, V = u(y)i, T = T(y) \tag{5}$$

where i is the unit vector along the x-axis. The dimensional basic field equations that govern the flow and heat transfer of an incompressible conducting fluid are as follows:
Continuity equation:

$$\nabla . V = 0 \tag{6}$$

Momentum equation:

$$\rho(V.\nabla)V = \nabla.\tau + J \times B + g\beta^*(T - T_0) \tag{7}$$

Energy equation:

$$\rho C_P(V.\nabla)T = k\nabla^2 T + \tau.L + Q_0(T - T_0) \tag{8}$$

With displacement currents disregarded, the Maxwell equation and the generalized Ohm's law appropriate for the problem can be expressed as

$$\nabla . V = 0, \nabla \times B = \mu_m J, \nabla \times E = 0 \tag{9}$$
$$J = \sigma(E + V \times B) \tag{10}$$

In equations (7) to(10), $\rho$is the density;V is the velocity;J is the current density;B is the total magnetic field so that $B = B_0 + B$;b denotes the induced magnetic field;$\mu_m$represents the magnetic permeability; E pertains to the electric field; and σ is the electrical conductivity of the fluid. Moreover,T is the fluid temperature, and T_0, Q_0, C_P, and k are the reference temperature, internal heat generation coefficient, mass specific heat, and thermal conductivity, respectively. In view of the above-mentioned assumptions and for a particularly small magnetic Reynolds number approximation (in which induced magnetic field b can be disregarded), the magnetic body force can be expressed in the following form:

$$\begin{aligned} J \times B &= \sigma[B_0(V.B_0) - V(B_0.B_0)] \\ &= -\sigma {B_0}^2 V \end{aligned} \tag{11}$$

With Eq. (5), continuity equation (6) is satisfied. Therefore, the three scalar momentum equations from (7) are

$$\frac{\partial p}{\partial x} = \frac{d}{dy}S_{xy} - \sigma {B_0}^2 u' + g\beta^*(T - T_0) \tag{12}$$
$$\frac{\partial p}{\partial y} = \frac{d}{dy}S_{yy} \tag{13}$$

and

$$\frac{\partial p}{\partial z} = \frac{d}{dy}S_{zy} \tag{14}$$

As discussed extensively in [3], the physical components of the Cauchy stress tensor are given as

$$\begin{aligned} S_{xx} = \frac{1}{N}\Bigg\{ & \mu[(\lambda_4 + \lambda_7) - (\lambda_3 + \lambda_6) \\ & + 2(\lambda_1 + \lambda_2)]\left(\frac{du'}{dy'}\right)^2 \\ & + \mu[(\lambda_4 + \lambda_7)\alpha'_2 \\ & - \alpha'_1(\lambda_3 + \lambda_6) \\ & + 2(\alpha'_1\lambda_1 + \alpha'_2\lambda_2)]\left(\frac{du'}{dy'}\right)^4 \Bigg\} \end{aligned} \tag{15}$$

$$S_{xy} = \frac{1}{N}\left\{\mu\frac{du'}{dy'} + \mu\alpha'_1\left(\frac{du'}{dy'}\right)^3\right\} \tag{16}$$

$$\begin{aligned} S_{yy} = \frac{1}{N}\Bigg\{ & \mu[(\lambda_4 + \lambda_7) - (\lambda_3 + \lambda_6)]\left(\frac{du'}{dy'}\right)^2 \\ & + \mu[(\lambda_4 + \lambda_7)\alpha'_2 \\ & - \alpha'_1(\lambda_3 + \lambda_6)]\left(\frac{du'}{dy'}\right)^4 \Bigg\} \end{aligned} \tag{17}$$

where

$$\alpha'_1 = \lambda_1(\lambda_4 + \lambda_7) - (\lambda_3 + \lambda_5)(\lambda_4 + \lambda_7 - \lambda_2)\frac{\lambda_5\lambda_7}{2} \quad (18)$$

$$\alpha'_2 = \lambda_1(\lambda_3 + \lambda_6) - (\lambda_3 + \lambda_5)(\lambda_3 + \lambda_6 - \lambda_1)\frac{\lambda_5\lambda_6}{2} \quad (19)$$

and

$$N = 1 + \alpha'_2\left(\frac{du'}{dy'}\right)^2 \quad (20)$$

Incorporating the stress components in Eq. (16) in the absence of a pressure gradient into Eq. (12) yields the dimensional governing equations for the momentum equation:

$$\frac{d^2u'}{dy'^2} + \left[(3\alpha'_1 - \alpha'_2) + \alpha'_1\alpha'_2\left(\frac{du'}{dy'}\right)^2\right]\left(\frac{du'}{dy'}\right)^2\frac{d^2u'}{dy'^2} - \frac{\sigma {B_0}^2 u'}{\mu}\left[1 + \left(\frac{du'}{dy'}\right)^2\right]^2 + g\beta^*(T - T_0)\left[1 + \alpha'_2\left(\frac{du'}{dy'}\right)^2\right]^2 \quad (21)$$

Following Khan et al. [8], the heat balance equation, in the presence of heat source, is

$$k\frac{d^2T}{dy'^2} + S_{xy}\frac{du'}{dy'} + Q_0(T - T_0) \quad (22)$$

Substituting Eq.(16) into Eq. (22) yields

$$k\frac{d^2T}{dy'^2} + \mu\left\{\frac{1 + \alpha'_1\left(\frac{du'}{dy'}\right)^2}{1 + \alpha'_2\left(\frac{du'}{dy'}\right)^2}\right\}\left(\frac{du'}{dy'}\right)^2 + Q_0(T - T_0) = 0 \quad (23)$$

The boundary conditions for the velocity slip of viscous fluid were used by Hayat et al. [5] and are given as follows:

$$u'(y') = \beta'_1\frac{du'(y')}{dy'}, \quad T(y') = 0 \quad at\ y' = 0 \quad (24)$$

$$u'(y') = \beta'_2\frac{du'(y')}{dy'}, \quad T(y') = h \quad at\ y' = h \quad (25)$$

where u' is the x-component of fluid velocity,T is the fluid temperature,T_0 is the specific heat capacity, B_0 is the applied magnetic fluid, σ is the electrical conductivity,Q_0 is the internal heat generation,k is the thermal conductivity,β'_1,β'_2 are the slip coefficients, andα'_1,α'_2represent the material parameters.

The following non-dimensional variable and parameters are used to non-dimensionalize the governing equations and boundary conditions:

$$u' = \frac{u}{U}, y' = \frac{y}{h}, H^2 = \frac{\sigma {B_0}^2 h^2}{\mu}, \alpha'_{1,2} = \frac{\alpha_{1,2}U^2}{h^2}, Br = \frac{\mu v^2}{k(T_h - T_0)},$$

$$\Omega = \frac{(T_h - T_0)}{T_0}, Q = \frac{Q_0h^2}{k}, Gr = \frac{g\beta^*h^2(T_h - T_0)}{\mu U}, \beta'_{1,2} = \frac{\beta_{1,2}}{h}, \theta = \frac{T - T_0}{T_h - T_0}, N_s = \frac{E_{gen}h^2{T_0}^2}{k(T_h - T_0)^2} \quad (26)$$

Substituting Eq. (26) into Eqs. (21) and (23) to (25) produces the following equations:

Dimensionless momentum equation:

$$\frac{d^2u}{dy^2} + \left[(3\alpha_1 - \alpha_2) + \alpha_1\alpha_2\left(\frac{du}{dy}\right)^2\right]\left(\frac{du}{dy}\right)^2\frac{d^2u}{dy^2} - H^2u\left[1 + \left(\frac{du}{dy}\right)^2\right]^2 + Gr\theta\left[1 + \alpha_2\left(\frac{du}{dy'}\right)^2\right]^2 = 0 \quad (27)$$

Heat balance equation:

$$\frac{d^2\theta}{dy^2} + Br\left\{\frac{1 + \alpha_1\left(\frac{du}{dy}\right)^2}{1 + \alpha_2\left(\frac{du}{dy}\right)^2}\right\}\left(\frac{du}{dy}\right)^2 + Q\theta = 0 \quad (28)$$

Boundary conditions:

$$u(y) = \beta_1\frac{du(y)}{dy}, \quad \theta(y) = 0 \quad at\ y = 0 \quad (29)$$

$$u(y) = \beta_2\frac{du(y)}{dy}, \quad \theta(y) = 1 \quad at\ y = 1 \quad (30)$$

2.1 Entropy Generation

Entropy generation is directly associated with thermodynamics. Determining the rate of entropy generation in a given system is essential to optimizing energy for the effective operation of such system. The exchange of momentum and energy within fluid and at boundaries causes continuous entropy generation in the system. Bejan [17] presented the volumetric rate of entropy generation as follows:

$$E_{gen} = \frac{k}{{T_0}^2}\left(\frac{\partial T}{\partial y'}\right)^2 + \frac{\tau.L}{T_0} \quad (31)$$

One part of entropy generation is caused by the irreversibility due to heat transfer, and the other is caused by viscous dissipation.

$$E_{gen} = \frac{k}{{T_0}^2}\left(\frac{\partial T}{\partial y'}\right)^2 + \frac{1}{T_0}\frac{du'}{dy'}S_{xy} \tag{32}$$

Incorporating the stress components in Eq. (16), we obtain the following equation under the applied magnetic field:

$$E_{gen} = \frac{k}{{T_0}^2}\left(\frac{dT}{dy'}\right)^2 + \frac{\mu}{T_0}\left\{\frac{1+{\alpha'}_1\left(\frac{du'}{dy'}\right)^2}{1+{\alpha'}_2\left(\frac{du'}{dy'}\right)^2}\right\}\left(\frac{du'}{dy'}\right)^2 + \frac{\sigma {B_0}^2 u^2}{T_0} \tag{33}$$

Introducing the dimensionless quantities defined in Eq. (26) generates anentropy generation rate of

$$N_s = \left(\frac{d\theta}{dy}\right)^2 + \frac{Br}{\Omega}\left\{\frac{1+\alpha_1\left(\frac{du}{dy}\right)^2}{1+\alpha_2\left(\frac{du}{dy}\right)^2}\right\}\left(\frac{du}{dy}\right)^2 + H^2u^2 \tag{34}$$

Let

$$N_1 = \left(\frac{d\theta}{dy}\right)^2, N_2 = \frac{Br}{\Omega}\left\{\frac{1+\alpha_1\left(\frac{du}{dy}\right)^2}{1+\alpha_2\left(\frac{du}{dy}\right)^2}\right\}\left(\frac{du}{dy}\right)^2 + H^2u^2 \tag{35}$$

where N_1 represents the irreversibility due to heat transfer, and N_2 denotes the entropy generation due to viscous dissipation. To determine whether the entropy generation due to viscous dissipation dominates over the irreversibility due to heat transfer or vice versa, we define the ratio of irreversibility thus:

$$\phi = \frac{N_2}{N_1} \tag{36}$$

The entropy generation due to viscous dissipation dominates if $\phi > 1$, whereas the irreversibility due to heat transfer dominates if $0 \le \phi < 1$. If $\phi = 1$, both phenomena provide equal contributions.

The Bejan number (Be) is defined as

$$\phi = \frac{N_1}{N_S} = \frac{1}{1+\phi} \tag{37}$$

where $Be = 0$ indicates the limit at which fluid friction irreversibility dominates,$Be = \frac{1}{2}$ signifies that both the entropy generation due to viscous dissipation and the irreversibility due to heat transfer contribute equally, and $Be = 1$ denotes the limit at which heat transfer irreversibility dominates.

The problem is now reduced to solve the non-dimensional boundary value problem governed by Eqs. (27) to (30). The solution is derived using the method of weighted residuals (MWR).

3. Solution Method

3.1 Principle of the MWR

The MWR is an approximation technique used to solve differential equations. It is categorized into various sub-methods, among which partitioning is one. This approach has been discussed by Aregbesola [24], Ghesemi et al. [25], Ledari et al. [26], and Odejide and Aregbesola [27].The basic principle of the MWR is to seek an appropriate polynomial solution to the boundary value problem of the form

$$D\big(u(y)\big) = p(y), \quad B(u) = \psi \; on \; \delta\Omega \tag{38}$$

where D is the differential operator acting on a function u to produce a known function p. Operator D can be a linear or non-linear expression of the spatial derivatives of dependent variable u. $B(u)$ denotes the appropriate boundary conditions, and Ω is a domain with boundary $\delta\Omega$.

Function u is approximated by a function U (i.e., a solution), which is represented as the linear combination of the basis function chosen from a linearly independent set, such that

$$u \cong U = \sum_{i=0}^{n} c_i y^i \tag{39}$$

where$c_i$are constants to be determined. U is sometimes called a trial function and is chosen in such a way that it satisfies all the boundary conditions of differential equations. Substituting Eq.(39) into the D in Eq. (39), whose result is generally not exactly equal to function $p(y)$, generates a residual or an error, such that

$$E(y) = R(y) = D\big(U(y)\big) - p(y) \neq 0 \tag{40}$$

The idea of MWR is to ensure that residual function $R(y)$ is as small as possible in some average sense over the domain. That is,

$$\int_{\delta\Omega} R(y)W_i dy = 0, \;\; i = 1,2,3 \ldots n \tag{41}$$

where the number of weight functions W_i is exactly equal the number of unknown constants $c_i$in$U$. This process translates to minimizing Eq.(41). The partition method is then used to minimize the residual function. The resultant systems of equations

are solved to determine parametersc_i. The polynomial U in Eq. (39) is the approximate solution.

The idea of partitioning is to force the weighted residual to zero not only at a fixed point in the domain but also over various subsections of the domain. To accomplish this, the weight functions are set to unity, and the integral over the entire domain is broken down into a number of partitions sufficient to evaluate all unknown parameters. That is,

$$\int_y R(y)W_i dy = \sum_i c_i \left(\int_{y_i} R(y)dy \right) = 0, \quad i = 1,2,3 \ldots n \tag{42}$$

3.2Application of the MWR to Equations

Consider the following trial solutions for the momentum equation:

$$\begin{aligned} u(y) = {} & \left(-\frac{y^6(5\beta_2 - 1)}{6\beta_2 - 1} + y^5 \right) a_5 \\ & + \left(-\frac{y^6(4\beta_2 - 1)}{6\beta_2 - 1} + y^4 \right) a_4 \\ & + \left(-\frac{y^6(3\beta_2 - 1)}{6\beta_2 - 1} + y^3 \right) a_3 \\ & + \left(-\frac{y^6(2\beta_2 - 1)}{6\beta_2 - 1} + y^2 \right) a_2 \\ & + \left(-\frac{y^6(-\beta_1 + \beta_2 - 1)}{6\beta_2 - 1} + y \right. \\ & \left. + \beta_1 \right) a_1 \end{aligned} \tag{43}$$

Similarly, for the heat balance equation, we assume

Note that Eqs. (43) and (44) satisfy the boundary conditions mentioned in Eqs. (29) and (30). Substituting $u(y)$ and $\theta(y)$ into Eq. (27) and (28) leads to residual functions $R_1(a_i, c_i, y)$ and$R_2(a_i, c_i, y)$as follows:

$$\begin{aligned} \theta(y) = {} & y^6 + c_1(y - y^6) + c_2(y^2 - y^6) \\ & + c_3(y^3 - y^6) \\ & + c_4(y^4 - y^6) \\ & + c_5(y^5 - y^6) \end{aligned} \tag{44}$$

$$\begin{aligned} R_1(a_i, c_i, y) = {} & 30y^4 - 30c_1y^4 + c_2(-30y^4 + 2) + c_3(30y^4 + 6y) \\ & + c_4(-30y^4 + 12y^2) + c_5(-30y^4 + 20y^3) \\ & + Br\left[\left(1 + \alpha_1 \left(-\frac{6y^5(5\beta_2 - 1)}{6\beta_2 - 1} + 5y^4 \right) a_5 \right. \right. \\ & + \left(-\frac{6y^5(4\beta_2 - 1)}{6\beta_2 - 1} + 4y^3 \right) a_4 \\ & + \left(-\frac{6y^5(3\beta_2 - 1)}{6\beta_2 - 1} + 3y^2 \right) a_3 \\ & + \left(-\frac{6y^5(2\beta_2 - 1)}{6\beta_2 - 1} + 2y \right) a_2 \\ & \left. \left. + \left(-\frac{6y^5(-\beta_1 + \beta_2 - 1)}{6\beta_2 - 1} + 1 \right) a_1 \right)^2 \right] \\ & / \left(1 + \alpha_2 \left(-\frac{6y^5(5\beta_2 - 1)}{6\beta_2 - 1} + 5y^4 \right) a_5 \right. \\ & + \left(-\frac{6y^5(4\beta_2 - 1)}{6\beta_2 - 1} + 4y^3 \right) a_4 \\ & + \left(-\frac{6y^5(3\beta_2 - 1)}{6\beta_2 - 1} + 3y^2 \right) a_3 \\ & + \left(-\frac{6y^5(2\beta_2 - 1)}{6\beta_2 - 1} + 2y \right) a_2 \\ & \left. + \left(-\frac{6y^5(-\beta_1 + \beta_2 - 1)}{6\beta_2 - 1} + 1 \right) a_1 \right)^2 \\ & + Q[y^6 + c_1(y - y^6) + c_2(y^2 - y^6) + c_3(y^3 - y^6) \\ & + c_4(y^4 - y^6) + c_5(y^5 - y^6)] \end{aligned} \tag{45}$$

$$\begin{aligned} R_2(a_i, c_i, y) = {} & \left(30\frac{y^4(5\beta_2 - 1)}{6\beta_2 - 1} + y^5 \right) a_5 + \left(30\frac{y^4(4\beta_2 - 1)}{6\beta_2 - 1} + y^4 \right) \\ & + \left(30\frac{y^4(3\beta_2 - 1)}{6\beta_2 - 1} + y^3 \right) a_3 + \left(30\frac{y^4(2\beta_2 - 1)}{6\beta_2 - 1} + y^2 \right) a_2 \\ & + 30\frac{y^4(-\beta_1 + \beta_2 - 1)}{6\beta_2 - 1} a_1 \\ & + \left(3\alpha_1 + \alpha_2 + \alpha_1\alpha_2 \left(6\frac{y^5(4\beta_2 - 1)}{6\beta_2 - 1} + 4y^3 \right) a_4 \right. \\ & + \left(6\frac{y^5(3\beta_2 - 1)}{6\beta_2 - 1} + 3y^2 \right) a_3 + \left(6\frac{y^5(2\beta_2 - 1)}{6\beta_2 - 1} + 2y \right) a_2 \\ & \left. + \left(6\frac{y^5(-\beta_1 + \beta_2 - 1)}{6\beta_2 - 1} + 1 \right) a_1 \right)^2 \left(\left(6\frac{y^5(5\beta_2 - 1)}{6\beta_2 - 1} + 5y^4 \right) a_5 \right. \\ & + \left(6\frac{y^5(4\beta_2 - 1)}{6\beta_2 - 1} + 4y^3 \right) a_4 + \left(6\frac{y^5(3\beta_2 - 1)}{6\beta_2 - 1} + 3y^2 \right) a_3 \\ & + \left(6\frac{y^5(2\beta_2 - 1)}{6\beta_2 - 1} + 2y \right) a_2 \\ & \left. + \left(6\frac{y^5(-\beta_1 + \beta_2 - 1)}{6\beta_2 - 1} + 1 \right) a_1 \right)^2 \left(\left(30\frac{y^4(5\beta_2 - 1)}{6\beta_2 - 1} + y^5 \right) a_5 \right. \\ & + \left(30\frac{y^4(4\beta_2 - 1)}{6\beta_2 - 1} + y^4 \right) a_4 + \left(30\frac{y^4(3\beta_2 - 1)}{6\beta_2 - 1} + y^3 \right) a_3 \\ & \left. + \left(30\frac{y^4(2\beta_2 - 1)}{6\beta_2 - 1} + y^2 \right) a_2 + 30\frac{y^4(-\beta_1 + \beta_2 - 1)}{6\beta_2 - 1} a_1 \right) \\ & - H^2 \left(\left(-\frac{y^6(5\beta_2 - 1)}{6\beta_2 - 1} + y^5 \right) a_5 + \left(-\frac{y^6(4\beta_2 - 1)}{6\beta_2 - 1} + y^4 \right) a_4 \right. \\ & + \left(-\frac{y^6(3\beta_2 - 1)}{6\beta_2 - 1} + y^3 \right) a_3 + \left(-\frac{y^6(2\beta_2 - 1)}{6\beta_2 - 1} + y^2 \right) a_2 \\ & \left. + \left(-\frac{y^6(-\beta_1 + \beta_2 - 1)}{6\beta_2 - 1} + y + \beta_1 \right) a_1 \right) \left(1 \right. \\ & + \alpha_2 \left(\left(6\frac{y^5(5\beta_2 - 1)}{6\beta_2 - 1} + 5y^4 \right) a_5 + \left(6\frac{y^5(4\beta_2 - 1)}{6\beta_2 - 1} + 4y^3 \right) a_4 \right. \\ & + \left(6\frac{y^5(3\beta_2 - 1)}{6\beta_2 - 1} + 3y^2 \right) a_3 + \left(6\frac{y^5(2\beta_2 - 1)}{6\beta_2 - 1} + 2y \right) a_2 \\ & \left. \left. + \left(6\frac{y^5(-\beta_1 + \beta_2 - 1)}{6\beta_2 - 1} + 1 \right) a_1 \right)^2 \right) \\ & + Gr\left(y^6 + c_1(y - y^6) + c_2(y^2 - y^6) + c_3(y^3 - y^6) \right. \\ & + c_4(y^4 - y^6) \\ & \left. + c_5(y^5 - y^6) \right) \left(1 \right. \\ & + \alpha_2 \left(\left(6\frac{y^5(5\beta_2 - 1)}{6\beta_2 - 1} + 5y^4 \right) a_5 + \left(6\frac{y^5(4\beta_2 - 1)}{6\beta_2 - 1} + 4y^3 \right) a_4 \right. \\ & + \left(6\frac{y^5(3\beta_2 - 1)}{6\beta_2 - 1} + 3y^2 \right) a_3 + \left(6\frac{y^5(2\beta_2 - 1)}{6\beta_2 - 1} + 2y \right) a_2 \\ & \left. \left. + \left(6\frac{y^5(-\beta_1 + \beta_2 - 1)}{6\beta_2 - 1} + 1 \right) a_1 \right)^2 \right) \end{aligned} \tag{46}$$

To determine unknown constants $a_i's$ and $c_i's$, each of the residuals is minimized using the partition method. Domain [0,1] is then divided into equal ranges. In particular, the sub-intervals below are chosen:

$$\left[0,\frac{1}{5}\right]\left[\frac{1}{5},\frac{2}{5}\right]\left[\frac{2}{5},\frac{3}{5}\right]\left[\frac{3}{5},\frac{4}{5}\right]\left[\frac{4}{5},1\right] \quad (47)$$

Simpson's rule is then applied on residuals $R(a_i, y)$ and $R(c_i, y), i = 1,2,3,4,5$ using the intervals in Eq. (47). A set of 10 equations and 10 unknown coefficients are obtained. The specific case for which $Br = 0.5, H = 0.1, Gr = 1, \beta_{1,2} = 0.1, \alpha_{1,2} = 0.2, Q = 0.5$ is considered.For this particular case, constants $a_i's$ and$c_i's$ are calculated thus:

$$\begin{aligned} a_1 = 0.1421108708,\ a_2 &= 0.00006404439119, a_3 \\ &= -0.2246142527, a_4 \\ &= 0.02066508321, a_5 \\ &= 0.005771203802, c_1 \\ &= 1.34942984, c_2 \\ &= -0.2500035733, c_3 \\ &= -0.1124250381, c_4 \\ &= 0.01033090181, c_5 \\ &= 0.002944291997 \end{aligned} \quad (48)$$

The approximate solutions of the equations are easily obtained by substituting the$a_i's$ and $c_i's$values derivedvia the partition method into the trial functions in Eqs. (43) and (44). These values are

$$\begin{aligned} u(y) = 0.01421108708 &+ 0.1421108708y \\ &+ 0.00006404439119y^2 \\ &- 0.2246142527y^3 \\ &+ 0.02066508321y^4 \\ &+ 0.005771203802y^5 \\ &- 0.0005419530775y^6 \end{aligned} \quad (49)$$

$$\begin{aligned} \theta(y) = 1.34942984y &- 0.2500035733y^2 \\ &- 0.1124250381y^3 \\ &+ 0.01033090181y^4 \\ &+ 0.002944291997y^5 \\ &- 0.000276430y^6 \end{aligned} \quad (50)$$

4. Graphical Illustration and Discussion

In this work, the effects of entropy generation on a viscoelastic Oldroyd 8-constant fluid in a vertical channel were investigated. The MWR was used to numerically solve the governing equations. The results of the MWR were compared with the numerical solutions obtained using the built-in package of MAPLE 18 for a Newtonian fluid (i.e., where $\alpha_1 = \alpha_2$) (Table 1). The package uses a fourth-order Runge–Kutta procedure. The error in Table 1 is defined as

$$Error = |u(y)_{Num} - u(y)_{Par}| \quad (51)$$

The results of the MWR are in good agreement with those of the MAPLE 18 package. To validate the code, we considered simplified versions of Eqs. (27), (28), and (30) by setting Gr and $\beta_1$to zero and setting $\beta_1 \frac{du}{dy}$ to unity. The resultant model is the same as the problem studied by Hayat et al. [3], that is, the steady plane Couette flow of an incompressible Oldroyd 8-constant fluid with no slip conditions. Hayat and his collaborators used homotopy analysis to solve the aforementioned problem. The comparison of the present results with those of Hayat et al. [3] is presented in Table 2. The table shows excellent correlation between the findings. Hence, confidence in the solutions derived through the present numerical method is high.

The convergence of the series solution obtained by partitioning weighted residuals is confirmed in Table 3. Given that this work focused primarily on entropy generation in a non-Newtonian Oldroyd fluid, the effects of various flow parameters on velocity, temperature, entropy generation, and the Bejan number were plotted graphically for the fluid (i.e., where $\alpha_1 \neq \alpha_2$). Fig. 2 depicts the effects of Hartmann number H on velocity. An increase in H reduces fluid velocity because of the retardation effect of Lorentz forces on flow. Velocity distribution is plotted against internal heat generation in Fig. 3. As observed from the plot, fluid velocity increases as internal heat generation parameter Q rises. This result can be attributed to the rise in fluid concentration.

Table1. Comparison of result for: $Br = 0.5, H = 0.1, Gr = 1, \beta_{1,2} = 0.1, \alpha_{1,2} = 0.2, Q = 0.5$

y	MWR	$Numerical$	$\lvert ERROR \rvert$
0.0	0.01421109	0.01433080	1.10^{-4}
0.1	0.02820116	0.02759609	6.00^{-4}
0.2	0.04087545	0.04063419	2.40^{-4}
0.3	0.05096823	0.05086193	1.10^{-4}
0.4	0.05727754	0.05706891	2.10^{-4}
0.5	0.05867025	0.05847328	1.90^{-4}
0.6	0.05408695	0.05397447	1.10^{-4}
0.7	0.04254700	0.04243647	1.10^{-4}
0.8	0.02315342	0.02328722	1.30^{-4}
0.9	−0.00490203	−0.00436217	5.30^{-4}
1	−0.04233395	0.04207047	2.60^{-4}

The influence of variations in internal heat generation parameter Q on temperature was also determined. An increase in Q increases the fluid temperature throughout the channel. Figs. 5 to 8 depict the effects of non-Newtonian parameters α_1 and α_2 on the velocity and temperature profiles. Fig. 5 indicates that an increase in α_1 reduces the velocity profile, and Fig. 6 shows that an increase in α_2 accelerates fluid velocity. This finding can be attributed to the shear thinning/thickening properties of the fluid. Fig. 7 reveals that under a variable α_1 and a constant α_2, the temperature profile increases. Fig. 8 shows that under a variable α_2 and a constant α_1, the temperature profile decreases. These

observations are due to the thickening/thinning phenomenon exhibited by the fluid.

Table2. Comparison of result for:$\alpha_{1,2} = 0.2, H = 2$

y	*Hayat et al.*[3]	*Present study*
0.0	0	0
0.25	0.143676	0.143676
0.5	0.324027	0.324027
0.75	0.587086	0.587086
1	1	1

Figs. 9 and 10 illustrate variations in the Brinkman number (Br) against the velocity and temperature profiles, respectively. The results show that an increase in Brinkman number increases both the velocity and temperature profiles because of the kinetic energy in the fluid.

Table 3. Convergence result for: $\alpha_{1,2} = 0.2, Q = 0.5, Br = 0.5, H = 0.1, Gr = 1, \beta_{1,2} = 0.1, y = 0.1$

n	u_n	$\sum_{n=0}^{6} u_n$	θ_n	$\sum_{n=0}^{6} \theta_n$
0	0.01421108708	0.0142111	0	0
1	0.1421108708	0.0284222	1.349429847	0.13494
2	0.00006404439	0.0284228	−0.25000357	0.13244
3	−0.2246142527	0.0286474	−0.112425040	0.13233
4	0.02066508321	0.0282003	0.0103309012	0.13233
5	0.0057712023802	0.0282003	0.0029442920	0.13233
6	−0.00054195308	0.0282003	−0.000276430	0.13233

Variations in slip parameters β_1 and β_2 and their effects on the velocity profile at the walls of the channel are displayed in Figs. 11 and 12, respectively. As β_1 increases, the fluid velocity in Fig. 11 rises at the wall with $y = 0$. However, a slightly reversed flow effect at the wall with $y = h$ also occurs. Fig. 12 indicates variations in slip parameter β_2 and their effects on fluid velocity. As slip parameter β_2 increases, fluid velocity decreases throughout the channel. The influence of the Grashof number (Gr) on the velocity profile is shown in Fig. 13. The plot demonstrates that an increase in Gr causes a corresponding increase in fluid velocity. This may be due to the fact that an increase in thermal buoyancy means a temperature difference in flow, which enhances fluid velocity.

Variations in various parameters for entropy generation are illustrated in Figs. 14 to 20. The effects of group parameter $Br\Omega^{-1}$ on the entropy generation rate are presented in Fig. 14. The plot shows that the entropy generation rate increases with increasing $Br\Omega^{-1}$ within the first width of the channel, but the reverse occurs within the remaining width of the channel. This phenomenon is due to the increase in the irreversibility N_2 of fluid friction with rising $Br\Omega^{-1}$ within half of the channel's width. A decrease in N_2 causes the reverse within the remaining width of the channel. Fig. 15 indicates the effects of Gr on the entropy generation rate, which increases as the Grashof parameter increases. This result is expected given that Gr increases the temperature profile (Fig. 13).

Figs. 16 and 17 illustrate the influence of non-Newtonian parameters α_1 and α_2 on the entropy generation rate. As presented in Figs. 7 and 8, an increase in α_1 and α_2 decreases fluid temperature. Parameter α_1 is expected to enhance the entropy generation rate, and $\alpha_2$is expected to decrease such rate. The effects of slip parameters β_1 and β_2 on the entropy generation rate are shown in Figs. 18 and 19. A slight increment occurs as both β_1 and β_2 increase. Fig. 20 reveals that an increase in Qelevates the entropy generation rate within the first half of the width of the channel and that a flow reversal takes place within the remaining width of the channel.

To examine the effects of different parameters on the Bejan number, we plotted related graphs in Figs. 21 to 28. Fig. 21 shows that an increasing H causes a decrease in the Bejan number, indicating that the irreversibility due to fluid friction is less dominant than heat transfer irreversibility. Figs. 22 and 23 depict variations in Gr and Q and their effects on the Bejan number, respectively. An increase in both Gr and Q indicates the strong dominance of fluid friction irreversibility over heat transfer irreversibility.

Figs. 24 and 25 illustrate the irreversibility ratio versus various values of α_1 and α_2. Asα_1 increases, fluid friction dominates over heat transfer irreversibility (Fig. 24), but as α_2 increases, heat transfer dominates over viscous dissipation (Fig. 25).Figs. 26 and 27 present the effects of slip variation parameters β_1 and β_2 on the Bejan number. As β_1 and $\beta_2$individually increase, fluid friction dominates over heat transfer irreversibility. Finally, the effects of $Br\Omega^{-1}$ on the Bejan number are depicted in Fig. 28, which shows that an increase in $Br\Omega^{-1}$ decreases the Bejan number. This result implies that the irreversibility due to heat transfer also decreases.

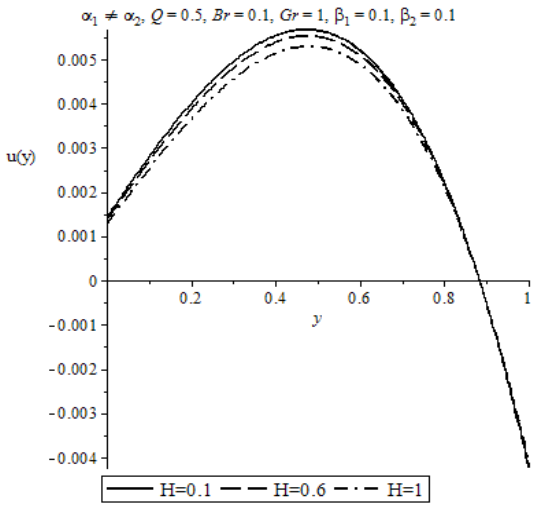

Fig. 2. Plot of velocity profile at different values of H

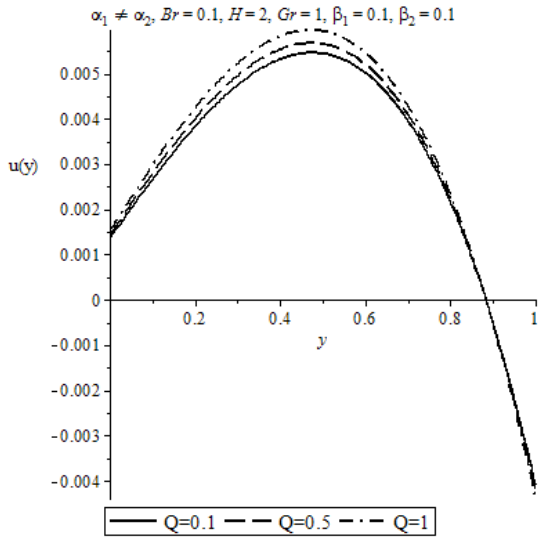

Fig. 3. Plot of velocity profile at different values of Q

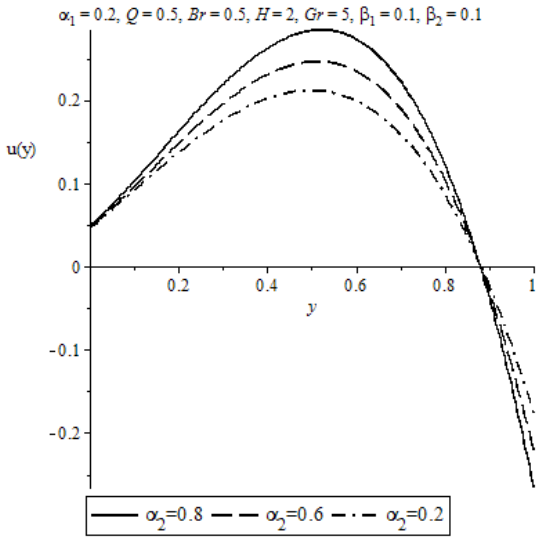

Fig. 6. Plot of velocity profile at different values of α_2

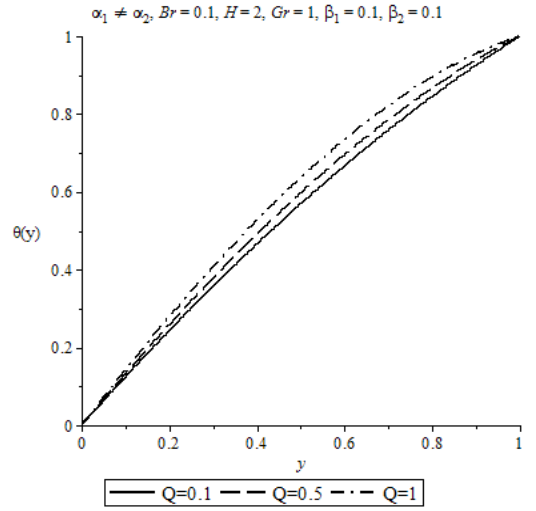

Fig. 4. Plot of temperature profile at different values of Q

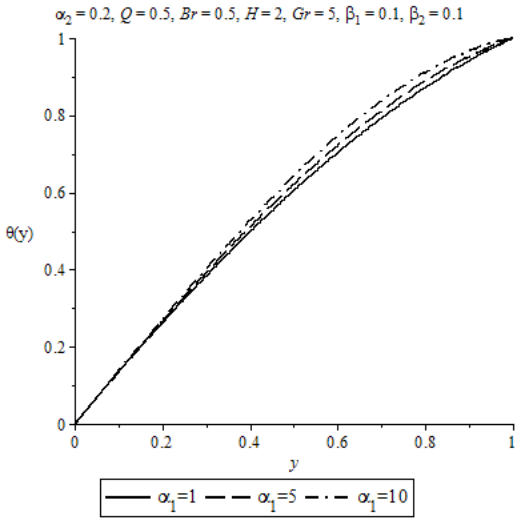

Fig. 7. Plot of temperature profile at different values of α_1

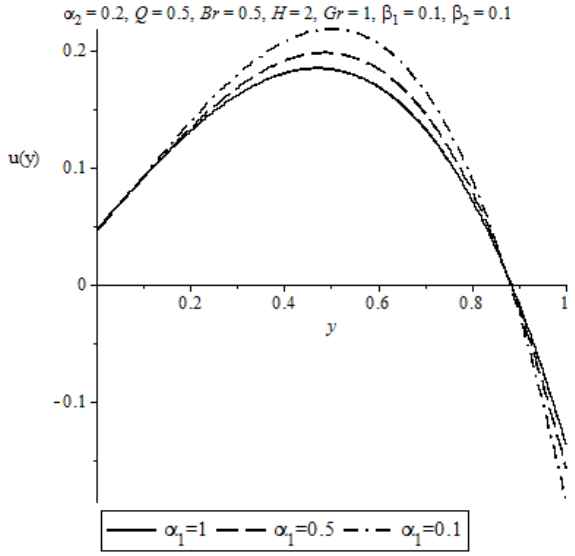

Fig. 5. Plot of velocity profile at different values of α_1

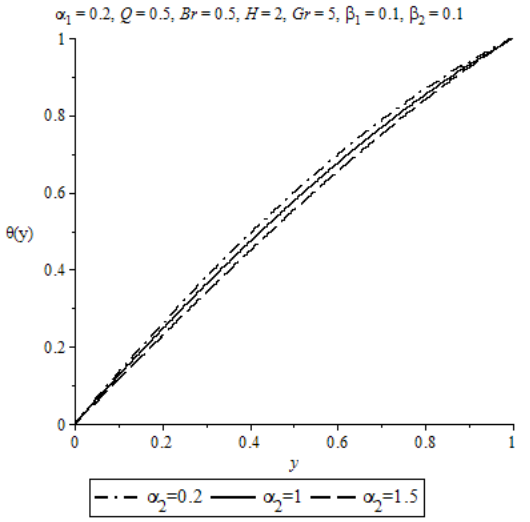

Fig. 8. Plot of temperature profile at different values of α_2

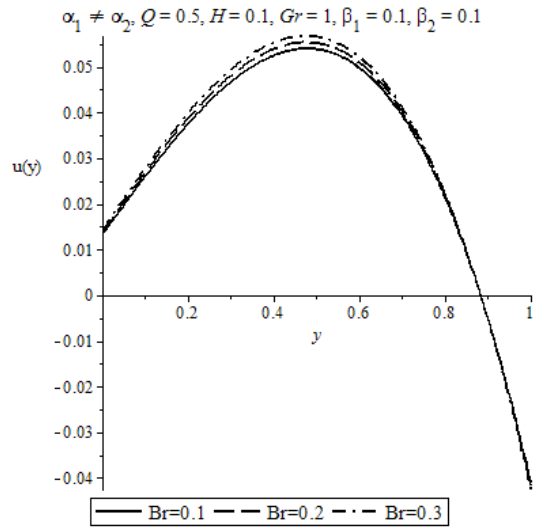

Fig. 9. Plot of velocity profile at different values of Br

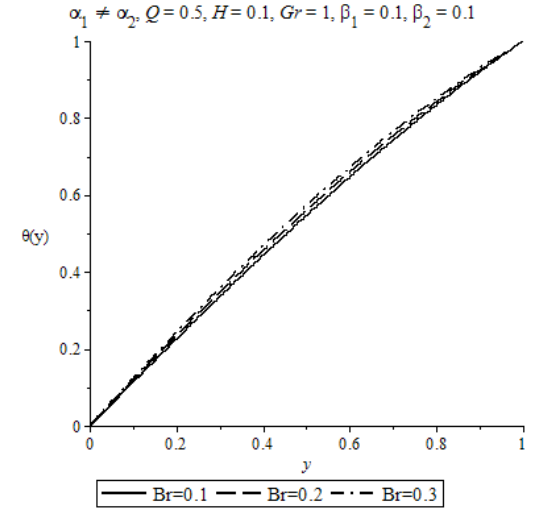

Fig. 10. Plot of temperature profile at different values of Br

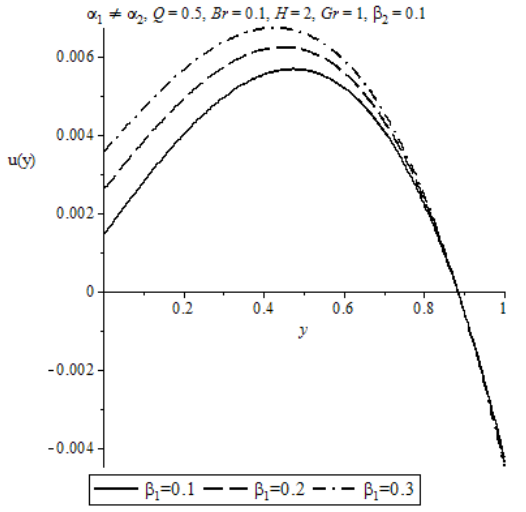

Fig. 11. Plot of velocity profile at different values of β_1

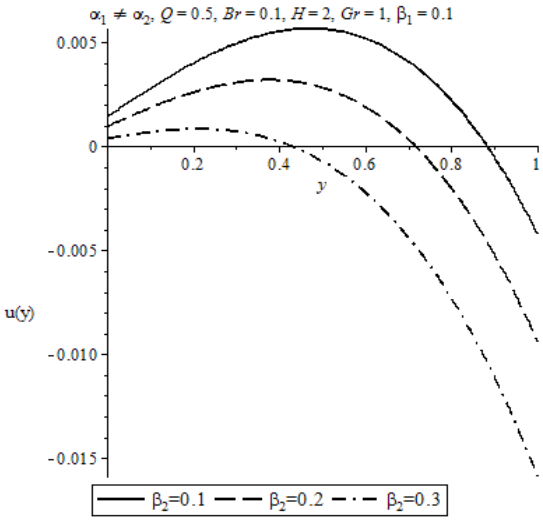

Fig. 12. Plot of velocity profile at different values of β_2

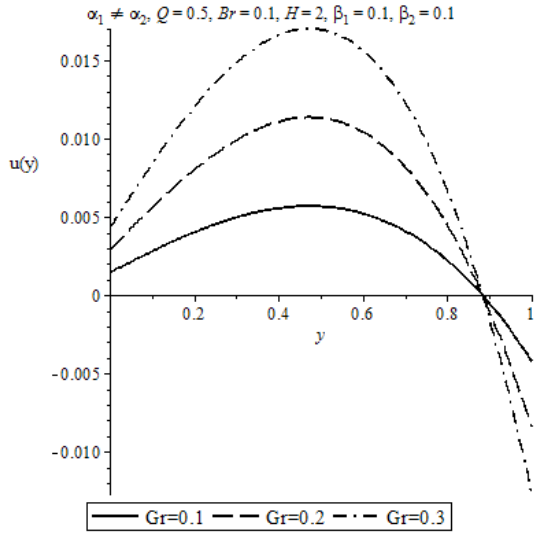

Fig. 13. Plot of velocity profile at different values of Gr

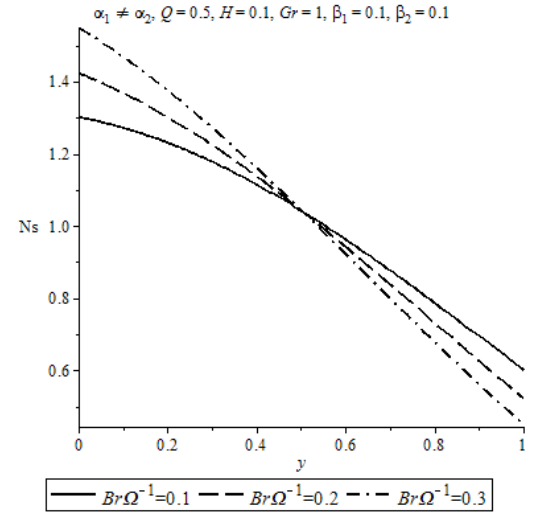

Fig. 14. Plot of entropy generation rate at different values of $Br\Omega^{-1}$

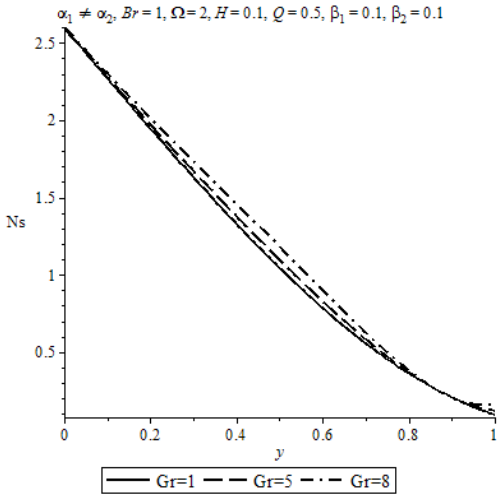

Fig. 15. Plot of entropy generation rate at different values of Gr

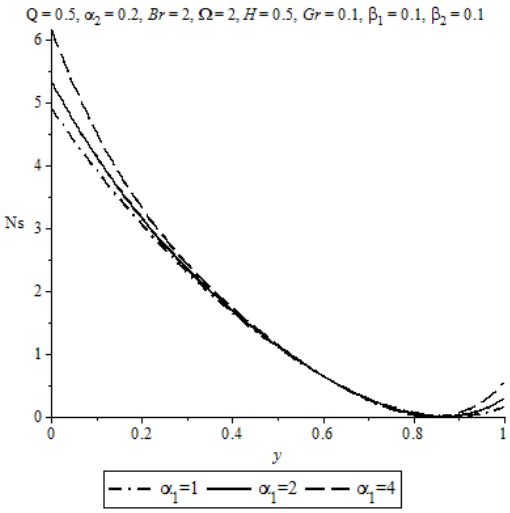

Fig. 16. Plot of entropy generation rate at different values of α_1

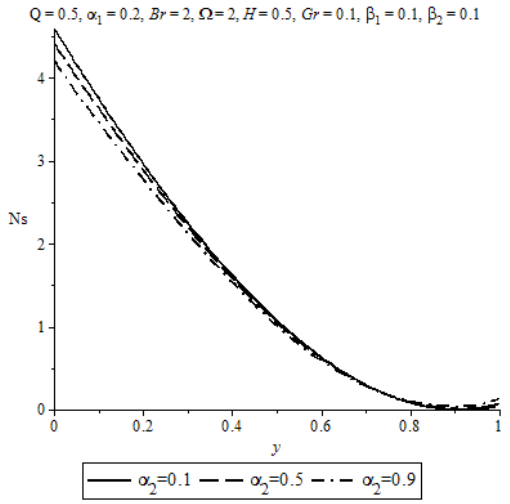

Fig. 17. Plot of entropy generation rate at different values of α_2

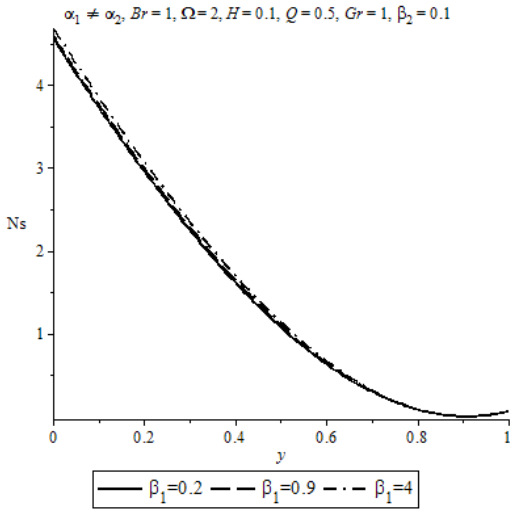

Fig. 18. Plot of entropy generation rate at different values of β_1

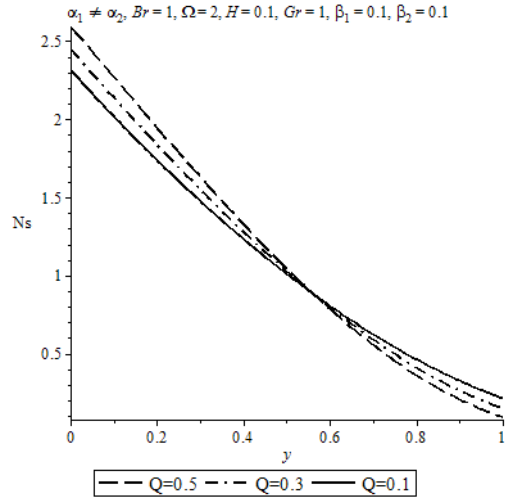

Fig. 20. Plot of entropy generation rate at different values of Q

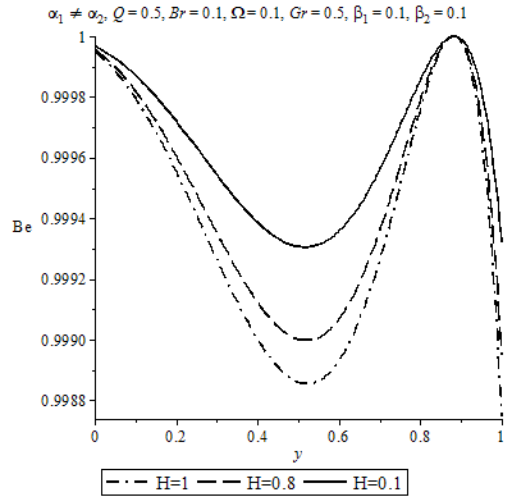

Fig. 21. Plot irreversibility ratio at different values of H

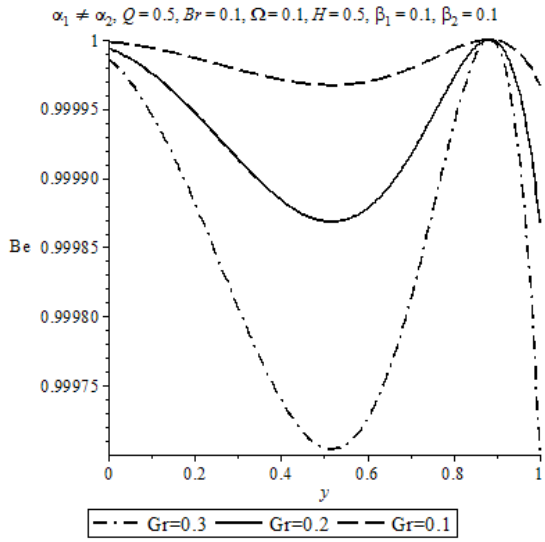

Fig. 22. Plot irreversibility ratio at different values of Gr

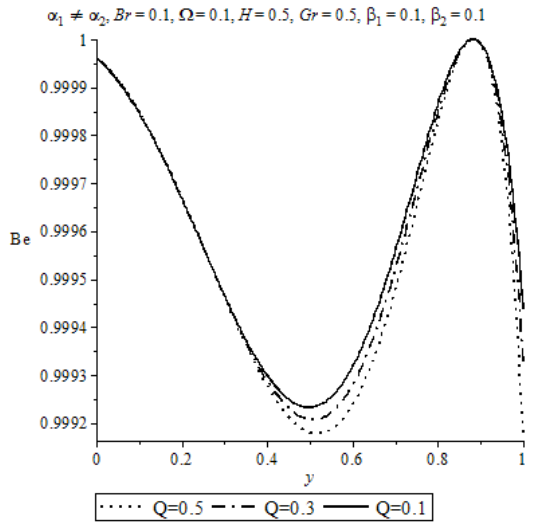

Fig. 23. Plot irreversibility ratio at different values of Q

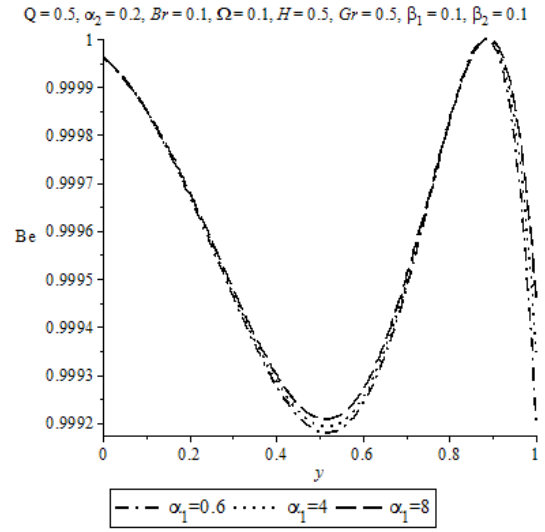

Fig. 24. Plot irreversibility ratio at different values of α_1

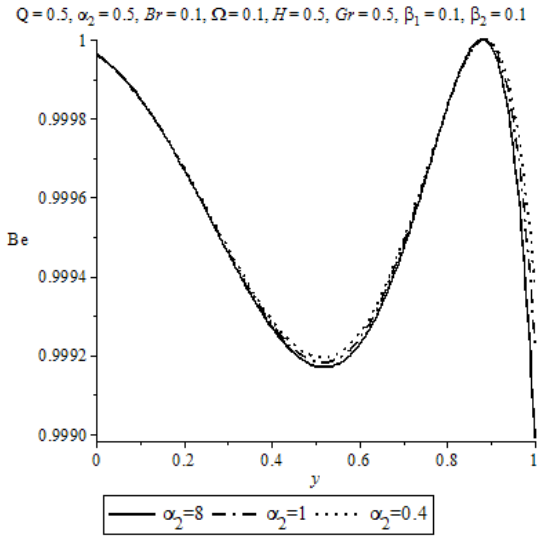

Fig. 25. Plot irreversibility ratio at different values of α_2

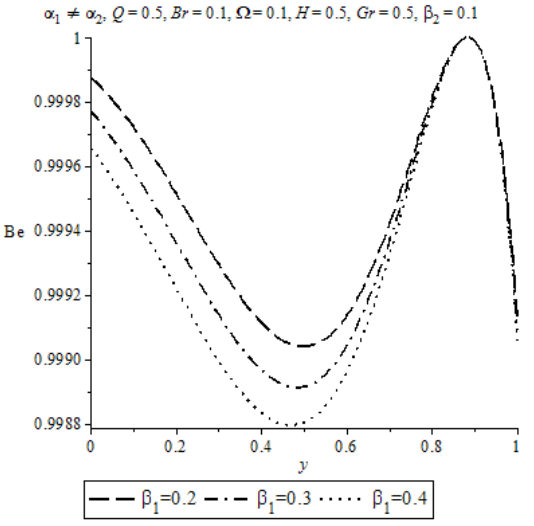

Fig. 26. Plot irreversibility ratio at different values of β_1

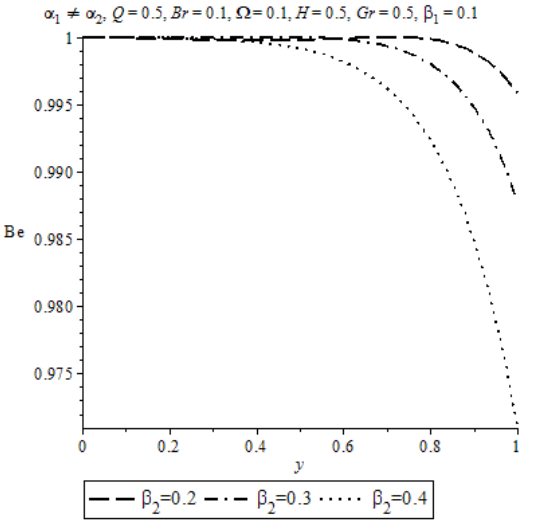

Fig. 27. Plot of irreversibility ratio at different values of β_2

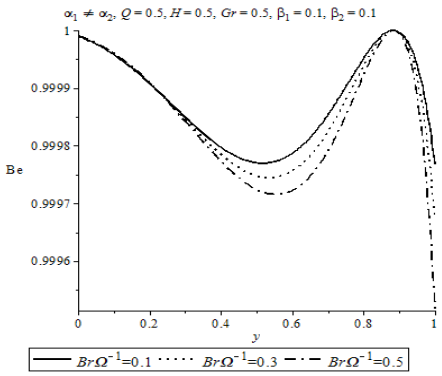

Fig. 28. Plot of irreversibility at different values of $Br\Omega^{-1}$

NOMENCLATURE

A_1	Rivlin–Ericksen tensor
H	Hartmannnumber
B_0	Magnetic field with constant strength
E_G	Entropy generation rate
N_S	Dimensionless entropy generation rate
T	Temperature (K)
T_0	Initial temperature (K)
T_h	Ambient temperature (K)
h	Channel width
u	Dimensionless velocity
u'	Dimensional velocity $(ms^{-1)}$
g	Acceleration due to gravity $(ms^{-2)}$
Q	Dimensionless internal heat generation
Q_0	Dimensional internal heat generation
y	Dimensionless position
y'	Dimensional position (m)
C_P	Specific heat at constant pressure $(J/kg\ K)$
k	Thermal conductivity
Gr	Grashof number
Be	Bejan number
Br	Brinkman number
S	Extra stress tensor
I	Identity tensor
$R_{1,2}$	Residuals

Greek symbols

β^*	Volumetric coefficient of thermal expansion
$\beta'_{1,2}$	Dimensional slip parameter
$\beta_{1,2}$	Dimensionless slip parameter
$\alpha'_{1,2}$	Dimensional non-Newtonian parameter
$\alpha_{1,2}$	Dimensionless non-Newtonian parameter
μ	Fluid viscosity $(kg\ m^{-1}s^{-1})$
σ	Electrical conductivity
ρ	Fluid density $(kg\ m^{-3})$
Φ	Irreversibility ratio
θ	Dimensionless temperature
Ω	Temperature difference parameter (K)
τ	Tensor stress
$\lambda_{1,2\ldots7}$	Material parameters

5. Conclusion

The effects of buoyancy and Navier slip on the entropy generation of an MHD Oldroyd 8-constant fluid in a vertical channel were investigated. The MWR was implemented to calculate the solutions of the momentum and thermal equation. The results were then used to compute the entropy generation rate and the irreversibility ratio. The core findings of the research are summarized as follows:

1. Velocity increases with rising magnetic parameter$H$.
2. When non-Newtonian parameters increase, shear thickening and shear thinning properties are reflected by both fluid velocity and fluid temperature.
3. Entropy generation increases at the wall with $y = 0$when the internal heat generation parameter and the group parameter increase. The reverse occurs at $y = h$.
4. The irreversibility due to fluid friction dominates over heat transfer when α_1 is kept constant at various values ofα_2, whereas the irreversibility due to heat transfer dominates over fluid friction when α_2 is kept constant at various values ofα_1.

Reference

[1]. J.G, Oldroyd, ‘‘On the formulation of rheological equation of state’’, Proc. Roy. soc. Londo. A, 200, 523-541, (1950).

[2]. R.B. Bird, R.C. Armstrong, O. Hassager, ‘‘Dynamics of polymeric liquids’’, Fluid Mech.1, PP. 354, New York: Wiley, (1987).

[3]. T. Hayat, M. Khan, and S. Asghar, ‘‘Homotopy analysis of MHD flows of an Oldroyd 8-constant fluid’’, Acta Mechanica, 168, 213–232, (2004).

[4]. T. Hayat, M. Khan, S. Asghar, ‘‘Megnetohydrodynamic flow of an Oldroyd 6-constant fluid’’, Applied Mathematics and Computation, 155, 417-425, (2004).

[5].T. Hayat, M. Khan, M. Ayub, ‘‘Effect of slip condition on flow of an Oldroyd 6-constant fluid’’, Journal of computation and Applied Mathematics, 202, 402-413, (2007).

[6].R. Ellahi,T. Hayat, T. Javed, S. Asghar, ‘‘On the analytic solution of nonlinear flow problem involving Oldroyd 8-constant fluid’’, Mathematical and Computer Modeling, 48, 1191-1200, (2008).

[7].S. Baris, ‘‘Flow of an Oldroyd 8-constant fluid in a convergent channel’’, Acta Mechanica, 148, 47-127, (2001).

[8]. M. Khan, Qurrat-ul-Ain, M. Sajid, ‘‘Heat transfer analysis of the steady flow of an Oldroyd 8-constant fluid due to suddenly moved plate’’, Commun Nonlinear Sci Numer Simulat, 16, 1347-1355, (2011).

[9]. M. Khan, T. Hayat, M. Ayub, ‘‘Numerical study of partial slip on the MHD flow of an Oldroyd 8-constant

fluid'', Computers and Mathematics with Applications, 53, 1088-1097, (2007).

[10].M. Khan, T. Hayat, W. Wang, ''Slip effects on shearing flows in a porous medium'', Acta Mech Sin, 24, 51-59, (2008).

[11].S. Das, R.N, Jana, ''Entropy generation due to MHD flow in a channel with Navier slip'', Ain Shams Eng. J., 5, 575-584, (2014).

[12]. J.A. Gbadeyan, T.A. Yusuf, M.S Dada, J.O. Akinremi, ''Effects Of slippage and couple stresses on entropy generation in a porous channel filled with highly porous medium'', Ilorin Journal of Science 2(1), 48-67, (2015).

[13]. J.A. Gbadeyan, T.A. Yusuf, ''Second law analysis of radiative unsteady MHD fluid flow with partial slip and convective boundary cooling'', Asian Journal of Mathematics and computer research, 17(4), 212-236, (2017).

[14].A.S. Eegunjobi, O.D. Makinde, ''Combined effect of buoyancy force and Navier slip on entropy generation in a vertical porous channel'', Entropy, 14, 1028-1044, (2012).

[15].A. Bejan. ''Entropy generation minimization''. New York, NY, USA, (1996) CRC Press.

[16].A. Bejan. ''Second Law Analysis in heat transfer'', Energy Int J., 5(7), 21-23, (1980).

[17].A. Bejan. ''Second Law Analysis in heat transfer and thermal design'', Adv. Heat Transf., 15, 1-58, (1982).

[18]. P. Vyas, A. Rai, ''Entropy regime for radiation MHD Couette flow inside a channel with naturally permeable base'', International Journal of energy and Technology, 5(19), 1-9, (2013).

[19]. S.O Adesanya, S.O. Kareem, J.A. Falade and S.A. Arekete, ''Entropy generation analysis for a reactive couple stress fluid flow through a channel saturated with porous material'', Energy, 93, 1239-1245, (2015).

[20]. S.O. Adesanya, J.A. Falade, ''Thermodynamics analysis of hydromagnetic third grade fluid flow through a channel filled with porous medium'', Alexandria engineering journal, 54, 615-622, (2015).

[21]. S.O. Adesanya, ''Second law analysis for third-grade fluid with variable properties'', Journal of thermodynamics. Article ID 452168, 8 pages http://dx.doi.org/10.1155/2014/452168, (2014).

[22]. S.O. Adesanya, O.D. Makinde, ''Entropy generation in couple stress fluid through porous channel with fluid slippage'', Int J. Exergy 15(3), 344-362, (2014).

[23]. A.O. Ajibade, B.K. Jha, A. Omame, ''Entropy Generation Under the effects of suction/injection'' Applied Mathematical Modelling., 35, 4630-4046, (2011).

[24]. Y.A.S. Aregbesola, ''Numerical solution of Bratu problems using the method of weighted residuals'', Electronic Journal of Southern African Math. Sci. Association (SAMSA), 3, 1-7, (2003).

[25]. P.M. Ghesemi, M. Abbasi, M. Khaki, ''New Analytic Solution of MHD fluid flow of fourth grade fluid through the channel with slip condition via collocation method'', Int. J. Adv. Appl. Math and Mech., 2(3), 87-94, (2015).

[26].S.T. Ledari, H. Mirgolbabaee, D.D. Ganji, ''Heat transfer analysis of a fin with temperature dependent thermal conductivity and heat transfer coefficient'', New Trends in Mathematical Sciences. 3(2), 55-69, (2015).

[27].S.A. Odejide, Y.A.S. Aregbesola,''Applications of Method of Weighted Residuals to Problems with Infinite Domain'', Rom. Journ Phys., 56(2), (2011) 14-24, (2011).